Communication

Virus Crystals as Nanocomposite Scaffolds

Joshua C. Falkner, Mary E. Turner, Joan K. Bosworth, Timothy J. Trentler, John E. Johnson, Tianwei Lin, and Vicki L. Colvin

J. Am. Chem. Soc., **2005**, 127 (15), 5274-5275• DOI: 10.1021/ja044496m • Publication Date (Web): 22 March 2005

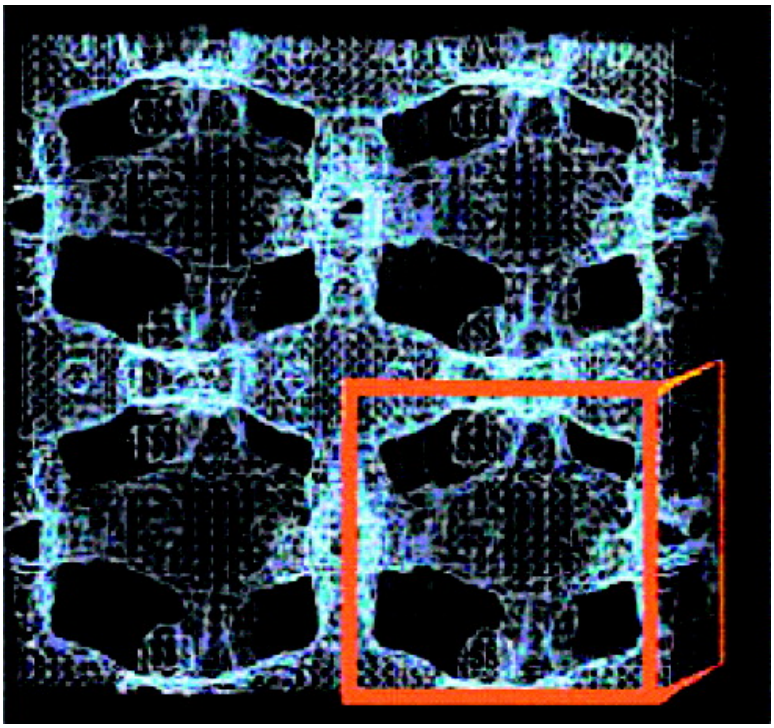

More About This Article

Additional resources and features associated with this article are available within the HTML version:

- Supporting Information
- Links to the 4 articles that cite this article, as of the time of this article download
- Access to high resolution figures
- Links to articles and content related to this article
- Copyright permission to reproduce figures and/or text from this article

J|A|C|S
COMMUNICATIONS

Published on Web 03/22/2005

Virus Crystals as Nanocomposite Scaffolds

Joshua C. Falkner,[†] Mary E. Turner,[†] Joan K. Bosworth,[†] Timothy J. Trentler,[†] John E. Johnson,[‡] Tianwei Lin,[‡] and Vicki L. Colvin*[,†]

MS-60, Department of Chemistry, Rice University, 6100 Main Street, Houston, Texas 77005, and MB-31, Department of Molecular Biology, The Scripps Research Institute, 10550 North Torrey Pines Road, La Jolla, California 92037

Received September 10, 2004; E-mail: colvin@rice.edu

Patterning the nanostructure of monolithic solids to make ordered motifs is a powerful tool for material design. Several chemical strategies for generating such materials rely on porous templates. Block copolymers and colloidal crystals are two such examples of templates used to generate long-range three-dimensional ordered materials.[1−3] While versatile in many ways, these templates offer only a limited number of architectures which can restrict their potential use. In particular, for optical applications crystal symmetries which are more complex than close-packed spheres or cylinders are required.[4] Biological templates, in contrast, provide a much wider variety of porous architectures and symmetries. Here we show that biological macromolecules in their crystalline state can be treated much like other monolithic templates and are effective at generating ordered solids of nanostructured materials.

Protein and virus crystals have traditionally played a pivotal role in structural biology where thousands of crystals with unique symmetries have been grown for macromolecular structure determinations.[5] However, it is only recently that macromolecular crystals have been exploited for noncrystallographic purposes as in the area of material synthesis.[6,7] An interesting and wide array of biological materials have been used as templates. Meldrum deposited gold onto sea urchin skeletal plates which were used to create micrometer-scale patterned materials.[8] Other studies have been performed on smaller biological systems such as DNA, microtubules, and individual virus particles to form metallic nanowires, nanofibers, and two-dimensional arrays of nanoparticles.[9−18]

In this work, we use virus crystals as templates to form large-scale solids containing nanoscopic order. The body centered cubic crystal of cowpea mosaic virus (CPMV) is used as an example template. This system has large nanoscopic cavities and channels (Figure 1A) which occupy about 50% of the crystal's total volume. These repeating channels within the CPMV crystals can be exploited as templates for the production of uniquely regular structures. We use the solvent channels of CPMV crystals to confine the growth of metals, including platinum and palladium. Metal infiltration into the mesoscopic channels of a three-dimensional lattice is a challenging process as it requires stringent reaction conditions and can be difficult to control for a homogeneous deposition. To address these issues, metal was deposited using an electroless plating process similar to that used to fill colloidal crystals and to coat microtubules.[10,13,19]

CPMV is an extensively studied virus that can be isolated in large quantities (over 1 g/kg of infected leaves) and crystallized using a straightforward procedure.[20] These body centered cubic crystals are reinforced by intervirus cross-linking so that they may be dried or exposed to a variety of solvents with little adverse effect on crystal quality.[6,21] We use a 10% glutaraldehyde as the cross-linking agent. The reinforced crystals are then exposed to a buffer that also contains 20 mg/mL potassium tetrachloropallidate(II). The palladium ions bind to basic amino acids that make up the protein shell or capsid of the virus particles in the crystals. The crystals are next placed in a buffer that contains 10 mg/mL potassium tetrachloroplatinate(II) hydrate and 20 mg/mL sodium hypophosphite. The catalytic cycle starts with the reduction of the coordinated Pd^{2+} by hypophosphite. This reduced Pd^0 completes the catalytic cycle by oxidizing and thereby reducing Pt^{2+} within the solvent channels of the crystals, producing virtually no reduced metal in solution.

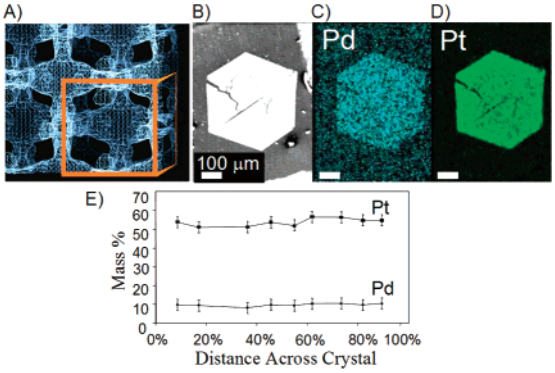

Figure 1. (A) Porous spaces between the viruses within the crystal structure, generated by XRD data. Orange box represents the unit cell. (B) SEM image of a cross-linked CPMV crystal after metallization. (C) X-ray backscattering of the palladium (D) and platinum distribution in the crystal. (E) EDX analysis of the metal distribution in the same crystal.

To ensure that the distribution of the metal throughout the virus crystal was uniform, we imaged cross sections of the crystal and analyzed micrometer-sized regions for their metal content. Metal-filled crystals were embedded in an epoxy matrix, Eponate-12 (Ted Pella), and approximately half of the crystal was removed with an ultramicrotome. The exposed microtomed, polished cross section was analyzed using a scanning electron microscope (SEM) equipped with an energy-dispersive X-ray (EDX) spectrometer. An SEM image and X-ray backscattering signal demonstrate the homogeneity of the metal distribution shown in Figure 1B, C, and D. This information was quantitated using EDX (Figure 1E) which found 10% Pd and 55% Pt by weight in the samples.

We confirmed that the formation of metals was confined to the channels of the virus crystal using electron microscopy. Thin cross sections (50−60 nm) were cut from metalized crystals using a Leica UCT-FCS ultramicrotome under cryogenic conditions. These cross sections were approximately 1.5−3.5 planes thick. Parts A and D of Figure 2 are transmission electron microscopy (TEM) images of typical lattice cross-sections cut near the (110) and (111) planes, respectively. B, C, E, and F of Figure 2 are simulations of how an *I*23 metal-infiltrated lattice would appear with those same orienta-

[†] Rice University.
[‡] The Scripps Research Institute.

10.1021/ja044496m CCC: $30.25

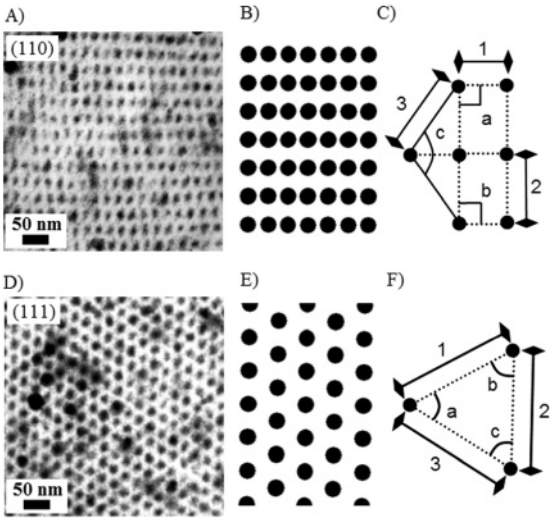

Figure 2. (A) TEM image of a thin (~50 nm) CPMV crystal cross-section. (B and C) Simulations of the metal-filled major pores along the (110) crystal plane of an *I*23 (body centered cubic) crystal. (D) TEM image of a thin (~50 nm) CPMV crystal cross-section. (E and F) Simulations of metal-filled major pores along the (111) crystal plane of an *I*23 (body centered cubic) crystal. The measured line segments and angles are listed in Table 1.

Table 1. Theoretical and Measured Lattice Features from Figure 2

	angle			segment		
	a (deg)	*b* (deg)	*c* (deg)	1 (nm)	2 (nm)	3 (nm)
(110)						
theoretical	90.0	90.0	109.1	15.9	22.4	27.5
measured	85.5	90.8	105.2	16.3	21.6	25.2
std. dev.	4.9	5.5	3.9	1.2	1.3	1.3
(111)						
theoretical	60.0	60.0	60.0	22.4	22.4	22.4
measured	62.8	52.2	60.7	21.5	17.8	21.5
std. dev.	4.0	2.9	3.4	1.2	1.4	1.2

tions and thicknesses. Table 1 gives the theoretical and measured values of segments and angles notated in Figure 2C and F. As indicated by Figure 2 and Table 1, these metal-infiltrated viruses retain their original crystalline structure.

Moreover, the angles and dimensions of the infiltrated lattice are near to those expected for a native lattice. We attribute the differences in these values to distortions that occur from crystal shrinkage during dehydration, as well as from the process of sectioning this brittle solid.

The lack of interconnects between the darker metal-filled portions of our composite (Figure 2) suggests that the templating process does not completely infiltrate the smaller porous sections to form one intact metal superstructure. In particular, it is more effective at generating metallic material in the larger portions of the porous network shown in Figure 1A and does not generally form metals between the areas of closest approach in the virus crystal. These metal-filled sections average 10.3 nm in diameter (Figure 2A, D), which compares favorably to the size of the larger compartments (Figure 1A) that are approximately 10−15 nm, depending on crystal orientation.

Further high-resolution studies of the metal portions find that this electroless deposition process forms metals that are nanostructured, consisting of single or aggregated nanocrystals ($d = 2.7$ nm). This result is in agreement with the metallic nanostructures found in similarly templated colloidal crystals, which also exhibited nanostructured crystallinity.[19] X-ray powder diffraction confirms the crystalline nature of the metal in the pores and through Scherrer analysis an average grain size of 1.3 nm was obtained.[22] We attribute the difference between the diffraction and imaged grain size to arise from the difficulty with measuring the precise size of the aggregated nanocrystals using TEM.

In summary, we have demonstrated that virus crystals can be used in material synthesis. They provide a porous, highly organized scaffold around which an inorganic matrix can be assembled. These nanocomposites, unlike the native virus or protein crystals, are sturdy materials. Moreover, they represent a monolithic three-dimensionally structured solid with nanometer-scale detail. These materials may find use as sensors and in X-ray optical systems.

Acknowledgment. This work was funded by National Science Foundation Grant (0103174 to V.C.) and Office of Naval Research (N00014-00-1-0671 to J.E.J. and N00014-03-1-0632 to T.L.). V.C. also thanks the Welch Foundation (C-1342) and the Beckman foundation for their support.

Supporting Information Available: Detailed Experimental Section describing the entire process and analysis. This material is available free of charge via the Internet at http://pubs.acs.org.

References

(1) Hashimoto, T.; Tsutsumi, K.; Funaki, Y. *Langmuir* **1997**, *13*, 6869−6872.
(2) Klok, H. A.; Lecommandoux, S. *Adv. Mater.* **2001**, *13*, 1217−1229.
(3) Martin, C. R. *Chem. Mater.* **1996**, *8*, 1739−1746.
(4) Colvin, V. L. *MRS Bull.* **2001**, 637−641.
(5) URL: http://www.rcsb.org/pdb/.
(6) Margolin, A. L.; Navia, M. A. *Angew. Chem., Int. Ed.* **2001**, *40*, 2204−2222.
(7) Flynn, C. E.; Lee, S. W.; Peelle, B. R.; Belcher, A. M. *Acta Mater.* **2003**, *51*, 5867−5880.
(8) Meldrum, F. C.; Seshadri, R. *Chem. Commun.* **2000**, 29−30.
(9) Dujardin, E.; Mann, S. *Adv. Mater.* **2002**, *14*, 775−788.
(10) Knez, M.; Sumser, M.; Bittner, A. M.; Wege, C.; Jeske, H.; Martin, T. P.; Kern, K. *Adv. Funct. Mater.* **2004**, *14*, 116−124.
(11) Wang, Q.; Lin, T.; Tang, L.; Johnson, J. E.; Finn, M. G. *Angew. Chem., Int. Ed.* **2002**, *41*, 459−462.
(12) Douglas, T.; Young, M. *Nature* **1998**, *393*, 152−155.
(13) Kirsch, R.; Mertig, M.; Pompe, W.; Wahl, R.; Sadowski, G.; Bohm, K. J.; Unger, E. *Thin Solid Films* **1997**, *305*, 248−253.
(14) Behrens, S.; Rahn, K.; Habicht, W.; Bohm, K. J.; Rosner, H.; Dinjus, E.; Unger, E. *Adv. Mater.* **2002**, *14*, 1621−1625.
(15) Mao, C. B.; Solis, D. J.; Reiss, B. D.; Kottmann, S. T.; Sweeney, R. Y.; Hayhurst, A.; Georgiou, G.; Iverson, B.; Belcher, A. M. *Science* **2004**, *303*, 213−217.
(16) Yan, H.; Park, S. H.; Finkelstein, G.; Reif, J. H.; LaBean, T. H. *Science* **2003**, *301*, 1882−1884.
(17) Mertig, M.; Wahl, R.; Lehmann, M.; Simon, P.; Pompe, W. *Eur. Phys. J. D* **2001**, *16*, 317−320.
(18) Hall, S. R.; Shenton, W.; Engelhardt, H.; Mann, S. *ChemPhysChem* **2001**, *2*, 184−186.
(19) Jiang, P.; Cizeron, J.; Bertone, J. F.; Colvin, V. L. *J. Am. Chem. Soc.* **1999**, *121*, 7957−7958.
(20) Lin, T.; Chen, Z.; Usha, R.; Stauffacher, C. V.; Dai, J.-B.; Schmidt, T.; Johnson, J. E. *Virology* **1999**, *265*, 20−34.
(21) Walt, D. R.; Agayn, V. I. *Trends Anal. Chem.* **1994**, *13*, 425−430.
(22) Stokes, A. R. Line Profiles. In *X-ray Diffraction of Polycrystalline Materials*; Peiser, H., Rooksby, H., Wilson, A., Eds.; The Institute of Physics: London, 1955; pp 409−429.

JA044496M